ISSN 2231-346X (Print)
JUSPS-A Vol. 33(6), 74-83 (2021). Periodicity-Monthly
Section A
ISSN 2319-8044 (Online)

JOURNAL OF ULTRA SCIENTIST OF PHYSICAL SCIENCES
An International Open Free Access Peer Reviewed Research Journal of Physical Sciences
website:- www.ultrascientist.org
Estd. 1989

Synthesis, Properties and Applications of Lead-Free Perovskites:A Review

SUNDAR SINGH[1*] and FAREED AHMAD[2]

[1*]Department of Physics, Bareilly College, Bareilly-243005 (India)
[2]Department of Applied Science and Humanities, Jamia Millia Islamia, New Delhi-110025 (India)
Corresponding Author Email: sundar_15singh@rediffmail.com
http://dx.doi.org/10.22147/jusps-A/330601

Acceptance Date 04th Octeber, 2021, Online Publication Date 07th October, 2021

Abstract

Perovskites are the materials or compounds having a structure similar to calcium titanium oxide ($CaTiO_3$). These materials possess the basic structure of ABX_3, in which A & B are the cations with +1 and +2 electron vacancy and X is an anion which may be either halogen or oxygen. Perovskites are chiefly being used in solar cells in the photo absorbing layer for solar to electrical energy conversion with relatively high efficiencies, besides their use in LEDs, photodetectors, X-ray detectors, lasers *etc*. The power conversion efficiency (PCE) of Perovskite solar cell (PSC) has increased from 10% in the year 2012 to 29.1% in 2020 and are promising to cross the theoretical maximum (Shockley-Queisser) limit of 33% for conventional silicon solar cells, besides having great thermal and mechanical stability values. Toxicity due to the presence of lead and associated instability of PSCs have led to the intensive research in lead-free perovskite solar cells (LF-PSCs). In this review article we have tried to explore the current status of synthesis, properties and applications of perovskites in PSCs, particularly lead-free perovskites, and will suggest future prospects in this widely attracted field of non-conventional energy generation.

Key words: Lead-free Perovskites, Power Conversion Efficiency, Charge Carrier Recombination, Electron Transport Layer, Hole Transport Layer.

1. Introduction

Perovskites have a general structure similar to the mineral calcium titanium oxide ($CaTiO_3$). This group of materials possess the basic structure of ABX_3, in which A & B are the cations and X is an anion that is either

a halogen or oxygen (fig. 1). The structure of perovskites contains the positively charged cations A and B present in the middle and at the corners of the cube respectively and the type X negatively charged anions smaller than A and B, present on the faces of the cube[1]. Type A organic cations may be methyl-ammonium (CH_3NH^{3+}) or formamidinium (NH_2CHNH^{2+}), type B inorganic cations like lead (Pb^{2+}), whereas X_3 halogen anion may be, in general, chloride (Cl^-) or iodide (I^-).

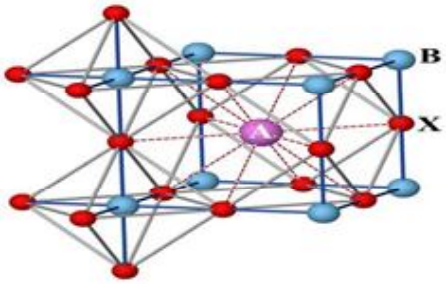

Figure 1: The ideal ABX_3 Perovskite Structure[1]

Initially the Perovskite materials were used in LEDs and in thin film transistors[2,3], but it was Miyasak and his group who first proved that Perovskites can be used for photovoltaic applications in the year 2006 and obtained a PCE of 2.2%. They synthesized $CH_3NH_3PbBr_3$ and used as an absorber material in a solar cell[4,5]. In 2009 by the same group Bromine (Br) was replaced with Iodine (I) to get $CH_3NH_3PbI_3$ as the perovskite absorber material in the fabricated PSC which enhanced PCE from 2.2% to 3.8%. Park and his co-researchers optimized perovskite solar cell by using mesoporous TiO_2 as electron transport layer (ETL) in 2011 and achieved significantly higher PCE of 6.5% [6,7]. In 2012 spiro-OMeTAD was used as the hole transport layer (HTL) by Park's and Gratzel's group and achieved a PCE of 9.7%. Seok's et al. achieved 12.3% PCE by using mix- halide Perovskite in 2013. In the same year, Gratzel et al. repeated the same work and increased the PCE to more than 15%. The Perovskite was for the first time deposited by Snaith et al by using vapor deposition technique in 2013. Various research groups were inspired and showed their interest in perovskites and repeated it to optimize the PCE of devices[8,9].

Of late, the chalcogenide perovskite, upgraded version of typical perovskite solar cell technology, have attracted the focus of the researchers for photovoltaics[10]. The chalcogenide perovskites with same chemical formula ABX_3, differ from general perovskites in that materials A and B represent the cations with +2 and +4 vacancies respectively and X represents the anions, chiefly S and Se. The cations of the B-site form octahedral coordination with the anions of the 6 X-site and form $[BX_6]$ n-octahedra in this structure. These octahedra form a three-dimensional framework by sharing their corners via X-site ions, resulting in a network of BXBX bonds in all three dimensions. The valence and conduction band borders of ABX_3 perovskites are mostly made up of these BX bonds[11-15]. As a result, the corner-shared octahedra govern the perovskite (ABX_3 primary)'s electrical and optical properties. These corner-shared octahedra create voids, which are subsequently occupied by A-site cations, who are in turn coordinated with 12 X-site ions to form a cuboctahedron. These A-site cations are instrumental in providing structural stability and charge neutrality, as well as the ability to impact the BX octahedral network and fine-tune optical and electrical properties[16-18].

2. Perovskite Solar Cell :

2.1 Structure of PSC: A PSC comprises of a metal electrode, an electron transporting layer (ETL), a light absorbing layer of perovskite material along with a mesoporous metal oxide (e.g., TiO_2), a hole transporting

layer (HTL) and a fluorine doped tin oxide (FTO) substrate[19-21]. Metal electrodes are made up of silver, gold or platinum and help in the collection of electrons and holes besides prohibiting charge carrier recombination. The ETL is basically made up of TiO_2. The TiO_2 transports electrons to the electrode; block holes and prevents the recombination at FTO substrate to increase the overall working efficiency of the solar cell[22]. The light absorbing layer of perovskite is embedded with porous and mesoporous metal oxide like zinc dioxide (ZnO_2), di-aluminium tri-oxide (Al_2O_3) and zirconium dioxide (ZrO_2). The photo catalytic generation of electron-hole pairs (EHPs) occurs here[23]. The HTL is generally made up of Spiro-OMeTAD or PEDOT: PSS which transports the generated holes and blocks electrons (fig. 2).

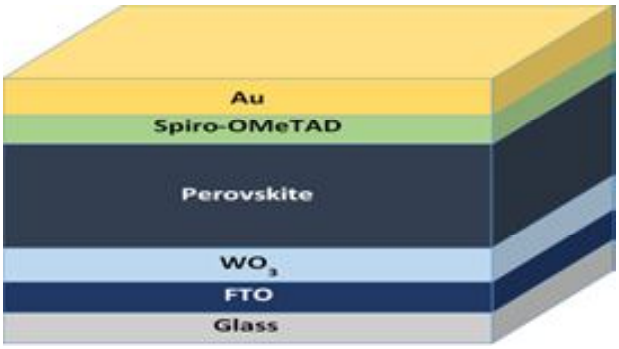

Fig. 2: Device Architecture of a planar PSC[24]

2.2 The Operating Principle of PSC: The perovskite layer in a PSC absorbs photons, creation of excitons follows (fig. 3). The creation of EHPs as a result of exciton dissociation occurs at the interface between the perovskite and the charge transport layer[25]. The produced charge carriers are subsequently delivered to their appropriate electrodes via the solar cell's transporting layers. Finally, they are removed and used to generate current in an external circuit[26-32].

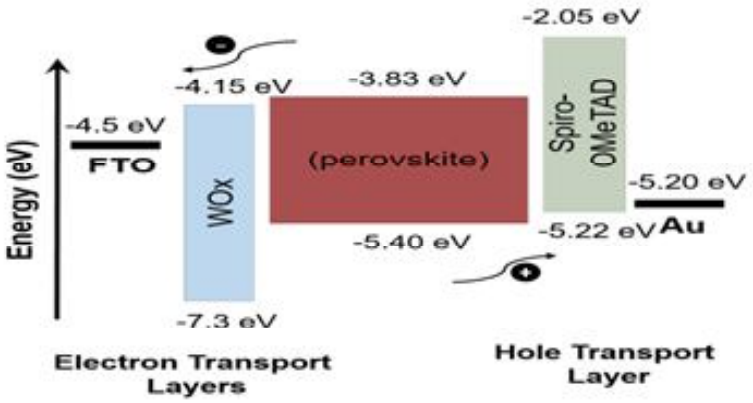

Figure 3: Operating Principle and Band Diagram of a PSC[24]

2.3 Lead-free Perovskites: PSCs possessing number of advantages also have certain drawbacks, notably the poor stability owing to moisture and heat, and toxicity due to the presence of lead. Contamination of lead ions to soil and water sources is of permanent nature and has a very harmful effect on human, animal and

plants. Environmental instability of PSCs is a serious issue that must be addressed. In 2016, Zhao *et al.* described the degradation of the perovskites in the presence of humidity or moisture in the environment and also showed the redox reactions to explain the solar cell degradation. Zhao and his coworkers also described that the metal used as back contact (metal contact) such as Al, Ag, Cr etc act as the catalyst which enhance the process of degradation. When PSCs are exposed in the sunlight under normal conditions, they start degradation due to the moisture present in the atmosphere[33,34]. When the Methyl ammonium lead iodide ($CH_3NH_3PbI_3$) comes in contact with moisture (H_2O molecules), it starts decomposition into CH_3NH_2, PbI_2 and HI by reacting with the H_2O molecules.

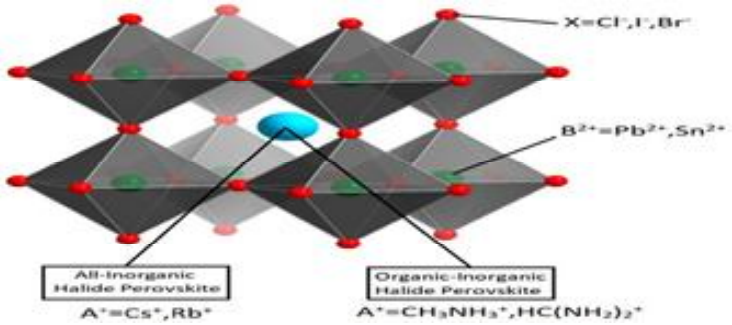

Figure 4: Schematic Diagram of ABX_3 Lead Halide Perovskite Structure[35]

To avoid toxicity associated with the use of lead, elements like Mg, Cu, Ag, Bi, and Sb may be used in place of lead in PSCs. Lead-free perovskites with chemical formula of the type $AB(II)X_3$, $A_2B(II)X_4$, AB (Ch, X)$_3$, $A_2B(I)B(II)X_6$ *etc* are used in PSCs.

3. Synthesis of Perovskites: The main hindrance to the large-scale commercial applications of lead-based halide perovskites in solar cells are their toxicity. So recently scientists have discovered a number of low to non-toxic varieties of perovskite materials which are not only lead-free but also quite environmentally friendly. Some of these perovskites display excellent optoelectronic properties along with device performances. Efficiency and stability are the two major concerns. So, such lead-free perovskites are being researched and developed possessing tunable optical and electrical properties. Their synthesis is of vital importance and there are various pathways to do so. Two such synthesis pathways (or methods) are discussed below.

3.1 Sequential Evaporation Method for Lead-Free Perovskite Thin Films: Qi *et.al.* developed a method to improve the quality of $MASnBr_3$-based perovskite film. $SnBr_2$ and MABr were used as the precursors and methods of co-evaporation and sequential evaporation were applied. In co-evaporation they used MABr/ $SnBr_2$ in the ratio of 4:1 and the two materials were simultaneously evaporated. This formed a perovskite film of 400 nm. But the PCE was low due to the oxidation of Sn^{2+} that hindered the generation of excitons along with blocking the carrier diffusion and final charge extraction. For this sequential evaporation was applied to reduce oxidation. First a 100 nm layer of $SnBr_2$ was deposited followed by a precipitation of a 400 nm film of MABr. The sample then was transferred to N_2 glovebox from vacuum for post annealing and the production of $MASnBr_3$ perovskite film. Hence a high-quality lead-free perovskite layer was produced[36].

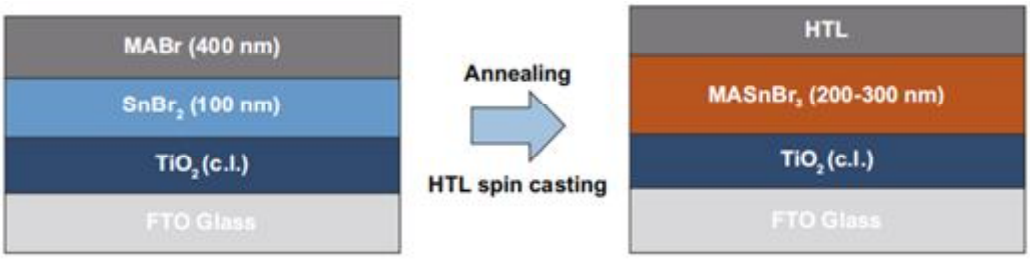

Figure 5: Sequential Evaporation Method to fabricate $MASnBr_3$ films[36]

3.2 Antisolvent Dropping Method for $Cs_2AgBiBr_6$ Perovskite: This method was developed by Wu *et. al*.[37]. In this method powdered $Cs_2AgBiBr_6$ was dissolved in a solution of dimethyl Sulphoxide (DMSO). Then it is spin-coated and annealed to get a lead-free double perovskite. The process is carried out under a low pressure of 20 Pa. It is followed by conventional annealing method where the transparent substrate film gradually turns to light yellow. Finally, the planar hetero-junction solar cell is obtained by using optimized $Cs_2AgBiBr_6$ perovskite film with poly(3-hexylthiopene) *i.e.*, P3HT as the HTL. Post annealing the films obtained had ultra-smooth morphology along with high crystallinity and micro-sized grains.

4. Properties of Perovskites :

4.1 Structural Properties: Double perovskites crystallize in cubic structure with space group *Fm*3*m* and can be represented by a general formula $A_2B'\ B''\ X_6$, where A atoms occupy the 8*c* Wyckoff position, B' atoms occupy the 4*a* Wyckoff position, B" atoms occupy the 4*b* Wyckoff position and X atoms occupy the 24*e* Wyckoff position with the fractional coordinates of (0.25, 0.25, 0.25), (0, 0, 0), (0.5, 0.5, 0.5) and (*x*, 0, 0), respectively. Initially, the structures of Cs-based inorganic double perovskites have been drawn, then the structures are converted into 1×1×1 supercell to get the structures of organic-inorganic hybrid double perovskites. The Cs-based inorganic double perovskites have 40 atoms in their unit cell with four formula unit. After creating supercell, the required Cs atoms have been successfully replaced by organic MA or FA to obtain the structures of the desired organic-inorganic hybrid double perovskites[38].

4.2 Electronic Properties: The electronic properties such as band gap and dielectric constants of double perovskites have been best illustrated through a comparison shown in fig. 6.

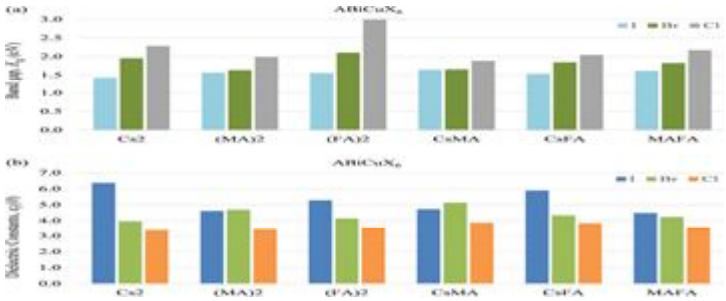

Figure 6: Comparison of the electronic band gap and dielectric constant of various double perovskites $ABiCuX_6$ [39]

4.3 Optical Properties: The optical properties for the double perovskites include dielectric function,

optical absorption, conductivity, reflectivity, refractive index and the extinction coefficient. The results suggest that the materials Cs_2BiCuI_6 and $(CsFA)BiCuI_6$ have higher dielectric constant at low energy region (from 0 to 2 eV). However, the double perovskite $(FA)_2BiCuI_6$ has maximum dielectric function at high energy region (from 2 to 4 eV) following a broad spectrum compared to other compounds. Also, the material $(FA)_2BiCuI_6$ shows the highest value of imaginary dielectric function compared to other compounds for solar radiation. The high value of dielectric function of $(FA)_2BiCuI_6$ for solar radiation implies that it is a promising candidate for photovoltaic applications. The materials show high absorption coefficient with a maximum absorption obtained with $(FA)_2BiCuI_6$. Therefore, the Pb-free organic-inorganic hybrid double perovskite $(FA)_2BiCuI_6$ are a potential alternative of Pb-based hybrid perovskites in solar cell application[39].

5. Applications of Perovskites :

5.1 Halide Double Perovskite for Solar Cells: Taking the advantages of Pb-free and excellent long-term stability into consideration, $Cs_2AgBiBr_6$ is expected to demonstrate extraordinary performance in optoelectronic, thermoelectric, ferroelectrics and so on. Among them, employing $Cs_2AgBiBr_6$ perovskite as the light-harvesting layer for LF-PSCs is current emphasis owing to their excellent photoluminescence lifetime (~ 660 ns) and tunable bandgap according to the researchers. Similar to state-of-the-art hybrid perovskites, Greul along with his coworkers prepared a high quality $Cs_2AgBiBr_6$ double perovskite film using one-step solution spin-coating technology by preheating and annealing treatments, and integrated it into solar cells for the first time.

5.2 LEDs: Till now, many materials have been employed to assemble LEDs, such as organic molecules, colloidal chalcogenide quantum dots and perovskite quantum dots owing to their narrow emission linewidth and tunable bandgap. However, organic molecules tailored devices generally display wide linewidth and the latter is limited by the toxicity of the cadmium and lead elements. Therefore, Pb-free perovskites are experimentally attempted to fabricate LED device. In 2016, Chao et al. firstly proposed a high-performance infrared LED based on low-temperature solution-processed $CsSnI_3$ perovskite. By optimizing the film quality, electroluminescence at 950 nm was obtained with maximum radiance of 40 W sr^{-1} m^{-2} at a current density of 364.3 mA cm^{-2} and maximum external quantum efficiency (EQE) of 3.8% at 4.5 V, demonstrating their feasibility for infrared lighting. Unfortunately, the oxidation of Sn^{2+} is also a challenge for stable LEDs. Inspired by photovoltaics, the 2D phenethyl ammonium tin iodide (PEA_2SnI_4) perovskite has been fabricated, showing an emission centered at 633 nm, which is ideal for red LED. Subsequently, Sargent *et al.* further incorporated H_3PO_2 into the perovskite film to suppress the oxidation pathway of Sn^{2+}, achieving an EQE of 0.3% and a brightness of 70 cd m^{-2}, which is the record among reported Pb-free red LEDs. Although great efforts have been achieved, these materials are still hindered by their oxidative instability. Therefore, exploring oxidatively stable and thermally robust phosphors is still required, such as Sb^{3+}, Bi^{3+} -based materials.

5.3 Photodetectors: Arising from their excellent optoelectronic properties, LFHPs is also suitable for ultraviolet-visible-near infrared (UV-Vis-NIR) PD devices owing to their tunable light-response region. So far, most researches on perovskite-based PDs are focused on the Pb-containing perovskite because of their success in solar cells. And for Pb-free PDs, the satisfactory results are still lacking, which are mainly based on Sn and double perovskites. For example, Waleed *et al.* fabricated a $MASnI_3$ nanowire-array based PDs with assistance of porous alumina template, achieving a responsivity and detectivity of only 0.47 A W^{-1} and 8.80×10^{10} Jones, respectively. However, the easy oxidization of Sn^{2+} to Sn^{4+} is also an undoubted factor that limits performance improvement. With the aim to resolve this issue, 2D PEA_2SnI_4 perovskite was fabricated and the corresponding

device demonstrated a responsivity of 16 A W^{-1}. Furthermore, adding SnX_2 and reducing agent can effectively stabilize the lattice and create a Sn^{2+} -rich environment to suppress the formation of Sn vacancy. In 2019, Yan et al. established an air-stable broadband response PD from ultraviolet to near-infrared light with a responsivity up to 105 A W^{-1} by introducing hydroxybenzene sulfonic acid additive along with excess $SnCl_2$ to encapsulate perovskite grains. Similarly, employing the same strategy (adding SnF_2 and ascorbic acid) can also improve the performance of $CsSnI_3$-based PDs.

Till now, the strategies to stabilize Sn-based perovskite lattice are still inspired from photovoltaics. In addition, VA group elements (*i.e*., Bi^{3+} and Sb^{3+}) are regarded as alternatives to assemble new Pb-free PDs. For example, zero-dimensional perovskites (N-methylpyrrolidinium)$_3Sb_2Br_9$ and (TMHD)$BiBr_5$ single crystals were discovered to show large spontaneous polarization as well as ultraviolet sensitive photoconductivity, demonstrating sizeable on/off current ratios ($\approx 10^3$) and rapid response speed around 10 ms. Comparing to the Sn and Pb based PDs, this kind of device generally demonstrates response to purple and ultraviolet light. It is well known that all-inorganic perovskites also show superior stability than hybrid species. In this fashion, $Cs_3Bi_2X_9$ has attracted more attention in photodetection applications recently. Pan et al. constructed PDs based on high-quality $Cs_3Bi_2I_9$ perovskite nanoplates by a facile solution-processed method, displaying maximum photoresponsivity of 33.1 mA/W and fast rise and decay time of 10.2 and 37.2 ms, respectively.

5.4 X-Ray Detectors: Bi-based perovskite is playing an important role in detecting X-rays due to its high carrier lifetime, high X-ray absorption coefficient and low ionization energy. Recently, Tang and co-workers synthesized high-quality $Cs_2AgBiBr_6$ single crystal through simple solution approach. By thermal annealing and surface treatment to eliminate Ag^+ /Bi^{3+} disorder and suppress ion migration, the optimized X-ray detectors achieved a high sensitivity of 105 μC Gyair $^{-1}cm^{-2}$ and a low detection limit of 59.7 nGyairs^{-1} at 5 V bias. The same group also employed bismuth oxybromide (BiOBr) as heteroepitaxial passivation layer to reduce trap density and suppress ionic migration in $Cs_2AgBiBr_6$ wafers, further increasing the performance with low noise (1/f noise-free), high sensitivity of 250 μC Gyair^{-1} cm^{-2}, and a spatial resolution of 4.9 lp mm^{-1}. Following this line of thought, high-quality perovskite films are very important to reduce material defects, suppress device noise and reduce leakage current, which is also suitable for $Cs_3Bi_2I_9$ and $MA_3Bi_2I_9$ based X-ray detectors. For example, Liu *et al.* developed a nucleation-controlled solution method to grow $Cs_3Bi_2I_9$ perovskite single crystals and Zhang et al. proposed a cold isostatic-pressing technology to fabricate $MA_3Bi_2I_9$ polycrystalline pellets, both demonstrating competitive advantages in practical applications.

5.5. Photocatalytic: Owing to their excellent photo-excited behavior and stability, Pb-free double perovskites have also shown potential application in photocatalytic area. Kuang's group has experimentally fabricated high quality $Cs_2AgBiBr_6$ nanocrystals via a traditional hot-injection approach and explored their application for photocatalytic CO_2 reduction. Arising from their structural stability in low polarity solutions up to three weeks, the $Cs_2AgBiBr_6$ nanocrystals achieved a total electron consumption of 105 μmol g^{-1} for CO_2 reduction reaction under AM 1.5G illumination for 6 h, displaying their great potential as environmentally friendly photocatalysts. And the photocatalytic ability can be further improved by introducing noble metals (Pt and Au) into the system. Beyond photocatalytic CO_2 reduction, the lead-free double perovskite $Cs_2AgBiBr_6$ also was applied for photocatalytic H_2 by Zhao and co-workers. Owing to the accelerated charge extraction and transfer from the reduced graphene oxide (RGO), the optimal $Cs_2AgBiBr_6$/2.5%RGO showed excellent photocatalytic performance and stability. Fabricating the metal/perovskite heterojunction to regulate the electronic distribution may be urgent to boost the development of perovskite as photocatalysts.

6. Conclusions

Despite the remarkable progress has been made in lead-based halide perovskites solar cells, the issue of lead toxicity still remains and inhibits further development. Undoubtedly, it is a good opportunity to develop lead-free perovskite materials, which is also an inevitable trend of commercial application in the coming years. However, there are many challenges in front of us, including low efficiency of LF-PSCs compared to Pb-based PSCs, poor film quality, serious charge carrier recombination, large electron and hole effective mass and wide or indirect bandgap. Notably, it is not easy to resolve all of these issues in just few years. We believe that many solutions will be proposed along with more and more researchers involving the techniques such as bandgap engineering, element doping, interfacial modification or surface-passivation, and the use of additives in the precursor solution and so on.

References

1. R. H. Mitchell, Nomenclature of the perovskite supergroup: A hierarchical system of classification based on crystal structure and composition, Mineralogical Magazine, *81(3),* 411–461 https://doi.org/10.1180/minmag. 2016.080.156 (2017).
2. Y. Peng, Q. Sun, H. Chen, and W. J. Yin, Disparity of the nature of the band gap between halide and chalcogenide single perovskites for solar cell absorbers. J. Phys. Chem. Lett., 2019., 10, 4566–70 https://doi.org/10.1021/acs.jpclett.9b01657
3. S. Niu *et al*., Bandgap control via structural and chemical tuning of transition metal perovskite chalcogenides, Adv. Mater., *29,* 16–21 https://doi.org/10.1002/adma.201604733 (2017).
4. A. Zakutayev *et al*., An open experimental database for exploring inorganic materials. Sci. Data, 2018., 5., 1–12 https://doi.org/10.1038/sdata.2018.5.
5. J. M. Frost and A. Walsh, What is moving in hybrid halide perovskite solar cells? Acc. Chem. Res., 2016., 49., 528–35 https://doi.org/10.1021/acs.accounts.5b00431.
6. R. Todorov, A. Paneva, K. Petkov, Optical characterization of thin chalcogenide films by multiple-angle-of-incidence ellipsometry, Thin Solid Films, 2010., 518(12)., 3280 http://dx.doi.org/10.1016/j.tsf.2009.09.002.
7. Z. Chaia et al., Synthesis of polycrystalline nanotubular Bi_2Te_3, Mater. Chem. Phys., 2009., 113, 664 http://dx.doi.org/10.1016/j.matchemphys.2008.07.121
8. S. Li *et al.*, Synthesis and assembly of monodisperse spherical Cu_2S nanocrystals., J. Colloid. Interface Sci., 2009., 330, 483 https://doi.org/10.1016/j.jcis.2008.10.062.
9. J. K. Dongre, V. Nogriya, M. Ramrakhiani, Structural, optical and photoelectrochemical characterization of CdS nanowire synthesized by chemical bath deposition and wet chemical etching., Appl. Surf. Sci., 2009., 255, 6115 http://dx.doi.org/10.1016/j.apsusc.2009.01.064
10. Z. H. Khan, G.L. Tan, J.H. Du, Q.J. Zhang, Structural evolution and optical properties of CdSe nanocrystals prepared by mechanical alloying., J. Alloys Compd., 2009., 468, 421 http://dx.doi.org/10.1016/j.jallcom.2008.01.051
11. Y. Yang, Y. Chai, D. Fanglin, Controllable synthesis of flower-like $Cd_{1-x}Zn_xSe$ microstructures from the self-prepared precursor., J. Alloys Compd., 2009., 478, 513 https://doi.org/10.1016/j.jallcom.2008.12.075
12. P.P. Ingole, P.M. Joshi, S.K. Haram, Room temperature synthesis of 1-hexanethiolate capped $Cu_{2-x}Se$ quantum dots in Triton X-100 water-in-oil microemulsions, *Colloids* Surf. A Physicochem. Eng. Aspects, 2009., 337, 136 http://dx.doi.org/10.1016/j.colsurfa.2008.12.011
13. S. Lee *et al*., Agarose and gellan as morphology-directing agents for the preparation of selenium nanowires in water., Carbohydr. Res., 2009., 344, 260 https://doi.org/10.1016/j.carres.2008.10.023
14. Q. Han *et al*., Synthesis of Sb_2S_3 peanut-shaped superstructures., Mater. Lett., 2009., 63, 1030 https://doi.org/10.1016/j.matlet.2009.01.078
15. K. Liu, H. Liu, J. Wang, L. Feng, Synthesis and characterization of $SnSe_2$ hexagonal nanoflakes., Mater.

Lett., 2009., 63, 512 http://dx.doi.org/10.1016/j.matlet.2008.10.054
16. Z. Li *et al*., Preparation of In_2S_3 nanoparticle by ultrasonic dispersion and its tribology property., Ultrason. Sonochem., 2009, 16, 221 https://doi.org/10.1016/j.ultsonch.2008.07.011
17. Y. Li, Y. Zhu, C. Li, X. Yang, C. Li, Synthesis of ZnS nanoparticles into the pore of mesoporous silica spheres., Mater. Lett., 2009., 63, 1068 https://doi.org/10.1016/j.matlet.2009.02.007
18. Z.H. Khan *et al*., Effect of composition on electrical and optical properties of thin films of amorphous Ga_xSe_{100-x}. Nanorods, Nano Res. Letts., 2010., 5, 1512 https://doi.org/10.1007/s11671-010-9671-5
19. Z.H. Khan, and M. Husain, Electrical and optical properties of thin film of a-$Se_{70}Te_{30}$ nanorods, J. Alloy. Compd., 2009., 486, 774 http://dx.doi.org/10.1016/j.jallcom.2009.07.049
20. R.M. Mehra, and P.C. Mathur, Analysis of single polaron hopping in ac conductivity of amorphous Ge20SbxSe80dx glasses, Thin Solid Films, 1989., 170, 15 https://doi.org/10.1063/1.343791
21. Mott N.F., and Davis E.A., (1979) *Electronic Processes in Non-crystalline Materials*, Clarendon, Oxford, p. 428 https://doi.org/10.1002/crat.19720070420
22. E.A. Davis, (1973) *Electronic and Structural Properties of Amorphous Semiconductors*, Academic Press, London, p. 425 https://doi.org/10.1016/0022-3093(81)90119-8
23. J. Nishi, S. Morimoto, I. Ingawa, R. Iizuka, T. Yamashita, Recent advances and trends in chalcogenide glass fiber technology: a review., J. Non-Crys. Solids, 1992., 140, 199 https://doi.org/10.1016/S0022-3093(05)80767-7
24. S. Mahjabin *et al*., Perceiving of Defect Tolerance in Perovskite Absorber Layer for Efficient Perovskite Solar Cell., IEEE Access, 2020, 1–1, https://doi.org/10.1109/access.2020.3000217
25. F.A. Agel, Optical and structural properties of a-Se_xTe_{100-x} aligned nanorods, Nanoscale Res. Lett., 2013., 8, 520 http://dx.doi.org/10.1186/1556-276X-8-520
26. Z.H. Khan *et al*., Electrical transport properties of a-Se87Te13 nanorods, J. Expt. Nanosci., 2010., 6, 337 https://doi.org/10.1080/17458080.2010.497946
27. S.A. Khan *et al*., Characterization of $Se_{88}Te_{12}$ nanostructured chalcogenide prepared by ball milling, Mater. Lett., 2010, 64, 1391 https://doi.org/10.1016/j.matlet.2010.03.035
28. A.A. Al-Ghamdi, S.A. Khan, A. Nagat, M.S. Abd El-Sadek, Synthesis and Optical characterization of nanocrystalline CdTe thin films, Opt. Laser Technol., 2010., 42, 1181 http://dx.doi.org/10.1016/j.optlastec.2010.03.007
29. S.A. Khan, F.A. Al-Agel, A.A. Al-Ghamdi, Optical characterization of nanocrystalline and chalcogenides, Superlattices Microstruct., 2010., 47, 695 http://dx.doi.org/10.1016/j.spmi.2010.03.007
30. N. Salah, S.S. Habib, A. Memic, N.D. Alharbi, S.S. Babkair, Z.H. Khan, Synthesis and characterization of thin films of $Te_{94}Se_6$ nanoparticles for semiconducting and optical devices, Thin Solid Films, 2013., 531, 70 https://doi.org/10.1016/j.tsf.2012.12.021
31. M.A. Alvi, and Z.H. Khan, Synthesis and characterization of nanoparticle thin films of a-$(PbSe)_{100-x}Cd_x$ lead chalcogenides, Nanoscale Res. Lett., 2013., 8, 148 https://doi.org/10.1186/1556-276X-8-148
32. N. Salah, S.S. Habib, Z.H. Khan, E. Alarfaj, S.A. Khan, Synthesis and characterization of $Se_{35}Te_{65-x}Ge_x$ nanoparticle films and their optical properties, J. Nanomater., 2012., 393084 http://dx.doi.org/10.1155/2012/393084
33. Z.H. Khan, A.A. Al-Ghamdi, S.A. Khan, S. Habib, N. Salah, Morphology and optical properties of thin films of Ga_xSe_{100-x} nanoparticles, Nanosci. Naotech. Lett., 2010., 3, 1 http://dx.doi.org/10.1166/nnl.2011.1188
34. Z.H. Khan, S.A. Khan, N. Salah, A.A. Al-Ghamdi, S. Habib, Electrical properties of thin films of a-Ga_xTe_{100-x} composed of nanoparticles, Phil. Mag. Lett., 2010., 93(7), 207 https://doi.org/10.1080/09500839.2010.547227
35. T. Dai *et al*., Strategies for High-Performance Large-Area Perovskite Solar Cells toward Commercialization, Crystals, 2021., 11(3), 295 https://doi.org/10.3390/cryst11030295
36. M.C. Jung, S.R. Raga, Y. Qi, Properties and solar cell applications of Pb-free perovskite films formed by

vapor deposition, RSC Adv., 2016., 6(4), 2819–2825 https://doi.org/10.1039/c5ra21291j

37. W. Gao, C. Ran, J. Xi, B. Jiao, W. Zhang *et al.*, High-quality $Cs_2AgBiBr_6$ double perovskite film for lead-free inverted planar heterojunction solar cells with 2% efficiency. ChemPhysChem, 2018., 19(14), 1696–1700 https://doi.org/10.1002/cphc.201800346
38. M. R. Filip et al., Band Gaps of the Lead-Free Halide Double Perovskites $Cs_2BiAgCl_6$ and $Cs_2BiAgBr_6$ from Theory and Experiment, The Journal of Physical Chemistry Letters, 2016., 7(13), 2579–2585 https://doi.org/10.1021/acs.jpclett.6b01041
39. M. Roknuzzaman *et al.*, Electronic and optical properties of lead-free hybrid double perovskites for photovoltaic and optoelectronic applications, Sci Rep, 2019., 9, 718 https://doi.org/10.1038/s41598-018-37132-2N
40. A. Guechi *et al.*, Elastic, Optoelectronic and Thermoelectric Properties of the Lead-Free Halide Semiconductors Cs_2AgBiX_6 (X = Cl, Br): Ab Initio Investigation, J. Electron Mater, 2018., 47, 1533–1545 https://doi.org/10.1007/s11664-017-5962-2
41. L. Dong *et al.*, Elastic Properties and Thermal Expansion of Lead-Free Halide Double Perovskite $Cs_2AgBiBr_6$, Comp. Mater. Sci, 2018., 141, 49-58 http://doi.org/10.1016/j.commatsci.2017.09.014
42. N. Rajeev Kumar, and R. Radhakrishnan, Electronic, Optical and Mechanical Properties of Lead-Free Halide Double Perovskites using First-Principles Density Functional Theory, Mater. Lett., 2018., 227, 289-291 https://doi.org/10.1016/j.matlet.2018.05.082
43. Y. Li *et al.*, Dimensional Reduction of $Cs_2AgBiBr_6$: 2D Hybrid Double Perovskite with Strong Polarization-Sensitivity, Angew. Chem. Int. Ed., 2020., 59, 3429-3433 https://doi.org/10.1002/anie.201911551
44. M. Pantaler et al., Hysteresis-Free Lead-Free Double-Perovskite Solar Cells by Interface Engineering, ACS Energy Lett., 2018., 3, 1781-1786 https://doi.org/10.1021/acsenergylett.8b00871
45. R. Kentsch *et al.*, Exciton Dynamics and Electron-Phonon Coupling Affect the Photovoltaic Performance of the $Cs_2AgBiBr_6$ Double Perovskite, J. Phys. Chem. C, 2018., 122, 25940-25947 https://doi.org/10.1021/acs.jpcc.8b09911
46. We. Ning *et al.*, Long Electron–Hole Diffusion Length in High-Quality Lead-Free Double Perovskite Films, Adv. Mater., 2018., 30, 1706246 https://doi.org/10.1002/adma.201706246
47. Z. Zhang *et al.*, Improvement of $Cs_2AgBiBr_6$ Double Perovskite Solar Cell by Rubidium Doping, Org. Electron, 2019., 74, 204-210 https://doi.org/10.1063/5.0059542
48. N. Pai *et al.*, Enhancement of the Intrinsic Light Harvesting Capacity of $Cs_2AgBiBr_6$ Double Perovskite via Modification with Sulphide, J. Mater. Chem. A, 2020., 8, 2008-2020 https://doi.org/10.1039/C9TA10422D
49. J. Li *et al.*, Alkali Metal Ion-Regulated Lead-free, All-Inorganic Double Perovskites for HTM-free, Carbon-Based Solar Cells, ACS Appl. Mater. Interfaces, 2020., 10.1021/acsami.0c11770. https://doi.org/10.1021/acsami.0c11770
50. T. Luo *et al.*, Dual Interfacial Engineering for Efficient Cs2AgBiBr6 Based Solar Cells, J. Energy Chem., 2021., 53, 372-378 https://doi.org/10.1021/acsami.0c09571
51. B. Wang *et al.*, Photoactive Zn-Chlorophyll Hole Transporter-Sensitized Lead-Free $Cs_2AgBiBr_6$ Perovskite Solar Cells, Sol. RRL, 2021., 4, 2000166 https://doi.org/10.1002/solr.202000166
52. G. Longo *et al.*, Understanding the Performance Limiting Factors of $Cs_2AgBiBr_6$ Double-Perovskite Solar Cells, ACS Energy Lett., 2020., 5, 2200-2207 https://doi.org/10.1021/acsenergylett.0c01020
53. T. L. Wu *et al.*, Diboron Compound-based Organic Light-emitting Diodes with High Efficiency and Reduced Efficiency Roll-off, Nat. Photonics, 2018., 12, 235-240 https://doi.org/10.1038/s41566-018-0112-9
54. X. L. Dai *et al.*, Solution-processed, High-performance Light-emitting Diodes based on Quantum Dots, Nature, 2014., 515, 96"99 https://doi.org/10.1038/nature13829
55. W. L. Hong *et al.*, Efficient Low-Temperature Solution-Processed Lead-Free Perovskite Infrared Light-Emitting Diodes, Adv. Mater., 2016., 28, 8029–8036 https://doi.org/10.1002/adma.201601024